JOURNAL OF BONE AND MINERAL RESEARCH
Volume 17, Number 4, 2002

Resistance to Unloading-Induced Three-Dimensional Bone Loss in Osteopontin-Deficient Mice

MUNEAKI ISHIJIMA,[1] KUNIKAZU TSUJI,[1] SUSAN R. RITTLING,[2] TERUHITO YAMASHITA,[1] HISASHI KUROSAWA,[3] DAVID T. DENHARDT,[2] AKIRA NIFUJI,[1] and MASAKI NODA[1]

ABSTRACT

Recent development in three-dimensional (3D) imaging of cancellous bone has made possible true 3D quantification of trabecular architecture. This provides a significant improvement in the measures available to study and understand the mechanical functions of cancellous bone. We recently reported that the presence of osteopontin (OPN) was required for the effects of mechanical stress on bone as OPN-null ($OPN^{-/-}$) mice showed neither enhancement of bone resorption nor suppression of bone formation when they were subjected to unloading by tail suspension. However, in this previous study, morphological analyses were limited to two-dimensional (2D) evaluation. Although bone structure is 3D and thus stress effect should be evaluated based on 3D parameters, no such 3D morphological features underlying the phenomenon have been known. To elucidate the role of OPN in mediating mechanical stress effect based on true quantitative examination of bone, we evaluated 3D trabecular structures of hindlimb bones of $OPN^{-/-}$ mice after tail suspension. Tail suspension significantly reduced 3D parameters of bone volume (BV/TV), trabecular number (Tb.N), trabecular thickness (Tb.Th), and anisotropy and increased 3D parameters on trabecular separation (Tb.Sp) in wild-type mice. In contrast, these 3D parameters were not altered after tail suspension in $OPN^{-/-}$ mice. These data provided evidence that OPN is required for unloading-induced 3D bone loss. (J Bone Miner Res 2002; 17:661–667)

Key words: osteopontin, mechanical stress, tail suspension, three-dimensional analysis, bone mineral density

INTRODUCTION

BONE RESORPTION and formation are under a balanced control to maintain bone mass. This balance is regulated not only by hormones and cytokines but also by mechanical stimuli.[1] For instance, loss of mechanical stress results in disruption of connectivity and the reduction in the number of trabecular bones to lead to osteopenia and thus significantly increases fracture risk in the bones composed primarily of trabecular structures such as vertebral body and femoral neck.[2] Similarly, strenuous exercise increases while microgravity reduces bone mass and strength.[3] Although these phenomena are well known, the underlying mechanisms have not yet been fully elucidated.

Osteopontin (OPN) is a secreted phosphoprotein present in extracellular matrix of mineralized tissues and is one of the abundant noncollagenous proteins in bone matrix produced by osteoblasts as well as osteoclasts.[4–6] This protein contains an arginine-glycine-aspartate (RGD) sequence that is a major integrin binding site and supports adhesion of bone cells to the mineralized matrix. Although OPN is expressed early in bone development, OPN per se is not

The authors have no conflict of interest.

[1]Department of Molecular Pharmacology, Medical Research Institute, Tokyo Medical and Dental University, Tokyo, Japan.
[2]Department of Cell Biology and Neuroscience, Rutgers University, Piscataway, New Jersey, USA.
[3]Department of Orthopedics, Juntendo University, School of Medicine, Tokyo, Japan.

required for the development of bones because these mineralized tissues are essentially normal in the OPN-null mice.[7–9] On the other hand, OPN plays an important role in the process of pathological bone resorption observed after ovariectomy or in the resorption of ectopically implanted bone discs.[10,11]

OPN expression is regulated by mechanical stress both in vitro and in vivo.[12–19] These observations could be related to the function of OPN in bone remodeling. However, the precise role of OPN in the regulation of bone response to the mechanical stress remains to be elucidated. Recently, we reported that unloading-induced enhancement of bone resorption and suppression of bone formation did not occur in the absence of OPN based on two-dimensional (2D) analyses of bone,[20] suggesting that OPN plays a key role in conveying the effect of mechanical stress to osteoclasts and osteoblasts.

Although bone structure should be evaluated in a 3D manner, which is not impossible but virtually very difficult, studies on the relationship between mechanical properties of bone and structure as well as bone mineral density (BMD) have been conducted based on conventional approaches such as histomorphometry.[21,22] Recent development in microcomputed tomography (μCT) imaging of cancellous bone could make 3D quantification of trabecular architecture more practical than before. Information on the 3D parameters is expected to provide precise evaluation on the mechanical features of cancellous bone.[23–26] However, no 3D parameter analyses were reported on the structural alteration in the cancellous bones in tail-suspended mice. Therefore, to truly determine the effect of OPN on unloading-induced bone loss, we conducted 3D analyses of the bones of wild-type and OPN$^{-/-}$ mice subjected to tail suspension.

MATERIALS AND METHODS

Animals

Female wild-type and OPN$^{-/-}$ mice in a 129/SV X C57BL/6 F2 background[8] derived from the original heterozygous crosses were maintained as separate colonies. These mice were kept under controlled conditions at 24°C on 12:12 light/dark cycles with the light cycle starting at 7:00 a.m., fed with standard laboratory chow (MF; Oriental Yeast, Tokyo, Japan) and given tap water. Twelve-week-old female OPN$^{-/-}$ and wild-type mice (24 mice total), 18–23 g of body weight, were used in the experiments and randomly assigned in equal numbers to loaded control and tail-suspension groups. All experiments were conducted according to the institutional guidelines for animal welfare.

Tail-suspension model

The mice were subjected to tail suspension as described previously.[20] Briefly, a tape was applied to the surface of the tail to set a metal clip. The end of the clip was fixed to the overhead bar and the height of the bar was adjusted to maintain in an ~30° head-down tilt with the hindlimbs elevated above the floor of the cage. Mice were permitted to move within the cage using their forelimbs while their hindlimbs were kept free of weight bearing. The mice in the unloading group were subjected to tail suspension for 4 weeks ($n = 6$/group). Loaded control mice were also housed individually under the same conditions except for tail suspension for 4 weeks. After 4 weeks of tail suspension, the mice were anesthetized with pentobarbital and were killed by cervical dislocation. The femora and tibias were separated from adherent muscles and connective tissues other than periosteum. The left tibias and the femora were fixed with 70% ethyl alcohol solution for subsequent analysis of bone.

Body weight of the animals

To monitor the effects of tail suspension on the general body condition of these animals, body weight was measured everyday during the experimental periods. When the mice were weighted, the tail-suspended mice were permitted to stand on all four legs for periods of no longer than 10 s.

Measurement of BMD

BMDs of the entire femora and the tibias including both proximal and distal ends as well as midcortical shafts were measured based on dual-energy X-ray absorptiometry (DXA) using an apparatus (PIXI; GE Lunar, Madison, WI, USA) equipped with a laptop computer. In vitro and in vivo coefficients of variation (%CV) were 0.5 and 0.87, respectively. The %CV was obtained by dividing the SD by the observed mean BMD (g/cm^2).

3D μCT analysis of bone

The bones were subjected to 3D μCT analysis using an algorithm equipped in a desktop 3D μCT system (μCT20; Scanco Medical AG, Zürich, Switzerland).[21,27] The spatial resolution is ~28 μm. Software based on an Image Processing Language (IPL; Institute for Biomedical Engineering, Swiss Federal Institute of Technology (ETH), and University of Zürich) package[28] equipped in the Scanco apparatus was used for the analysis of the parameters including bone volume (BV/TV, fractional bone volume), trabecular number (Tb.N), trabecular thickness (Tb.Th), trabecular separation (Tb.Sp), and anisotropy. The bone surface was calculated using surface triangulation of the binary data based on the marching cube method. The trabecular bone volume was calculated using tetrahedrons representing the enclosed volume of the triangulated surface used for the surface area calculation. The 3D bone volume was normalized against 3D total volume to obtain the fractional bone volume (BV/TV). Mean Tb.Th was determined based on the local thickness at each voxel representing bone. With this technique, thickness can be calculated without a model assumption. Tb.Sp was calculated by applying the same technique as used for the direct thickness calculation of the nonbone parts of the 3D image. The Tb.N was calculated by taking the inverse of the mean distance between the middle axes of the structure. The anisotropy was determined from the ratio between the maximal and minimal radii of the

mean intercept length (MIL) in the ellipsoid.[29] The MIL distribution was calculated by superimposing parallel test lines in different directions on the 3D image, where MIL denotes the mean distance between the bone/marrow interfaces. The MIL ellipsoid was calculated by fitting the MIL values to a directed ellipsoid.[21] Quantification of 3D analysis was made in the spherical area with a diameter of 0.54 mm, centered at 0.27 mm distal to the primary spongiosa of the proximal ends of the tibias. Threshold for the measurements was set at 275 for 3D analyses according to the manufacture's protocol.

Statistical evaluations

The results were presented as mean value ± SEM. Statistical analysis was performed by Mann-Whitney's *U*-test. A value of $p < 0.05$ was considered to be statistically significant.

RESULTS

3D analysis of the effects of OPN deficiency on unloading-induced bone loss

To examine 3D structural features of the effect of OPN deficiency on unloading-induced cancellous bone loss in $OPN^{-/-}$ mice, μCT-based analyses of the metaphyseal regions of the tibias were conducted. As presented in Fig. 1, 3D structures of the trabecular bone in the center of the metaphyseal region in the tibia of wild-type mice were lost after 4 weeks of tail suspension compared with the wild-type loaded group. In addition, trabecular bones adjacent to the endosteal surface of the metaphyses were disrupted in wild-type tail-suspended mice (Fig. 1). In contrast, 3D structures of the trabecular bones in the center as well as in the periphery in the endosteal regions of the metaphyses of the tibias in the tail-suspended $OPN^{-/-}$ mice were maintained and revealed similar features to those in loaded mice (Fig. 1, $OPN^{-/-}$ suspended vs. loaded).

Quantification of the 3D structures was conducted in a spherical area, which was just adjacent to the growth plate within the metaphyseal cancellous bone in the proximal ends of the tibias (Fig. 2A). Quantification of the 3D BV/TV indicated ~80% reduction by 4 weeks of unloading in wild-type mice ($p < 0.05$; Fig. 2B), whereas no major reduction was observed after unloading in $OPN^{-/-}$ mice (Fig. 2B). 3D Tb.N in the metaphyseal regions of the tibias was reduced by ~25% after 4 weeks of unloading in wild-type mice ($p < 0.05$; Fig. 2C), whereas such reduction was not observed in $OPN^{-/-}$ mice. Although ~80% reduction in the levels of 3D Tb.Th ($p < 0.05$; Fig. 2D) was observed in wild-type mice after 4 weeks of tail suspension, the values in tail-suspended $OPN^{-/-}$ mice were not significantly different from those in loaded $OPN^{-/-}$ mice (Fig. 2D). Furthermore,3D Tb.Sp was increased by 35% ($p < 0.05$; Fig. 2E) in wild-type mice because of unloading, but no significant increase was observed in $OPN^{-/-}$ mice after 4 weeks of tail suspension (Fig. 2E).

Anisotropy of the trabecular bones in the metaphyseal regions of the tibias of unloaded mice was reduced by 12% compared with that in loaded control after 4 weeks of unloading in wild-type mice ($p < 0.05$; Fig. 2F). On the other hand, no statistically significant difference was observed between loaded control and unloaded mice even after 4 weeks of tail suspension in $OPN^{-/-}$ mice (Fig. 2F).

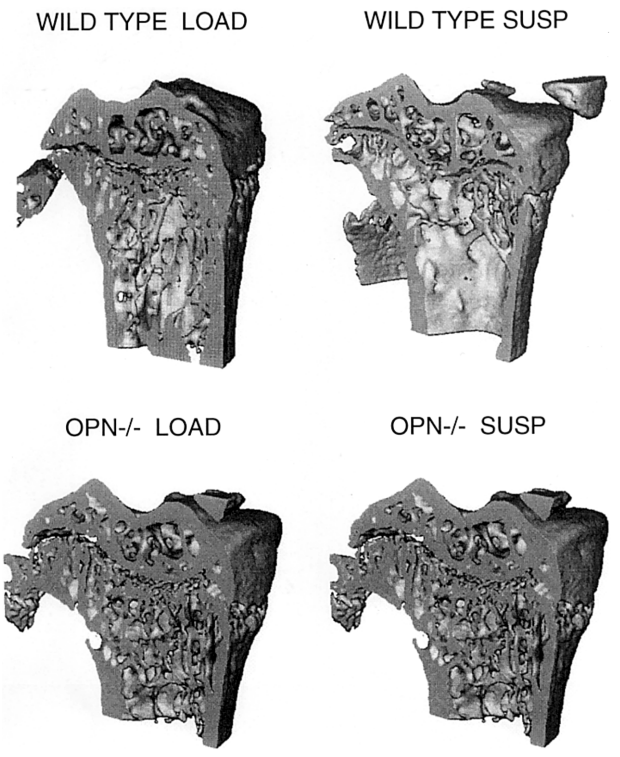

FIG. 1. 3D structures of the metaphyseal cancellous bones of the tibias. 3D views of the μCT pictures were obtained by scanning the proximal regions of the tibias after 4 weeks of tail suspension (SUSP) or loading (LOAD) in wild-type (WILD TYPE) or $OPN^{-/-}$ mice ($OPN^{-/-}$).

Unloading reduces BMD in wild-type mice but not in OPN-deficient mice

To examine whether these 3D structural changes could be translated into those in BMD, we examined the bones using DXA. In wild-type mice, BMD in the tibias was reduced by tail suspension for 4 weeks (Fig. 3A). Although the level of the BMD reduction in the whole tibias by tail suspension was modest, this possibly was caused by the incorporation of the BMDs in both epiphyseal ends as well as midshaft of the bones. Because of the limitation of the small size of the mouse bones and the resolution of the DXA apparatus, we were not able to segregate the data of epiphyseal regions versus those of the diaphysis. To confirm the observation in tibias, we also analyzed the BMD in femora. Similar to the observation in tibias, BMD in femora also was reduced in wild-type mice by tail suspension (Fig. 3B). In $OPN^{-/-}$ mice, the basal BMD levels in both femora and tibias of the loaded group were similar to those in the loaded wild-type group (Figs. 3A and 3B). However, in contrast to the

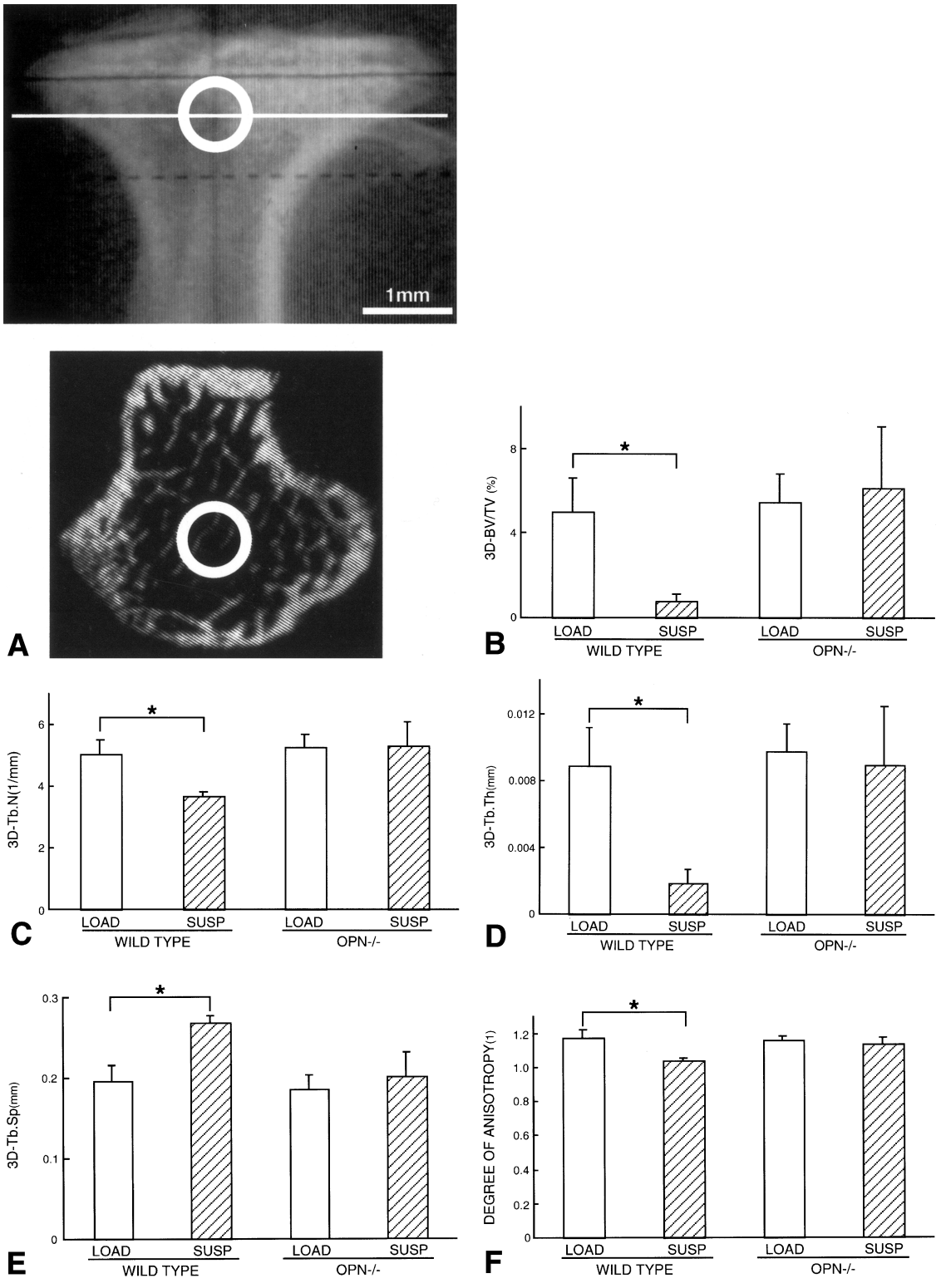

FIG. 2. 3D μCT analysis of the cancellous bone structures in tibias after 4 weeks of unloading. 3D-μCT analyses were conducted by scanning the proximal regions of the tibias after 4 weeks of tail suspension (SUSP) or loading (LOAD) in wild-type (WILD TYPE) or OPN$^{-/-}$ mice (OPN$^{-/-}$). (A) A simple X-ray scout view (top panel) and a μCT picture in the horizontal plane (bottom panel) of the proximal tibias. The circles shown in these panels indicate the spherical region where the 3D parameters of trabecular bone were quantified. (B) 3D BV/TV; (C) 3D Tb. N; (D) 3D Tb. Th; (E) 3D Tb.Sp; (F) anisotropy. These values were calculated as described in the Materials and Methods section. Data are expressed as means and SEs for wild-type and OPN$^{-/-}$ mice. *Statistically significant difference from respective control ($p < 0.05$).

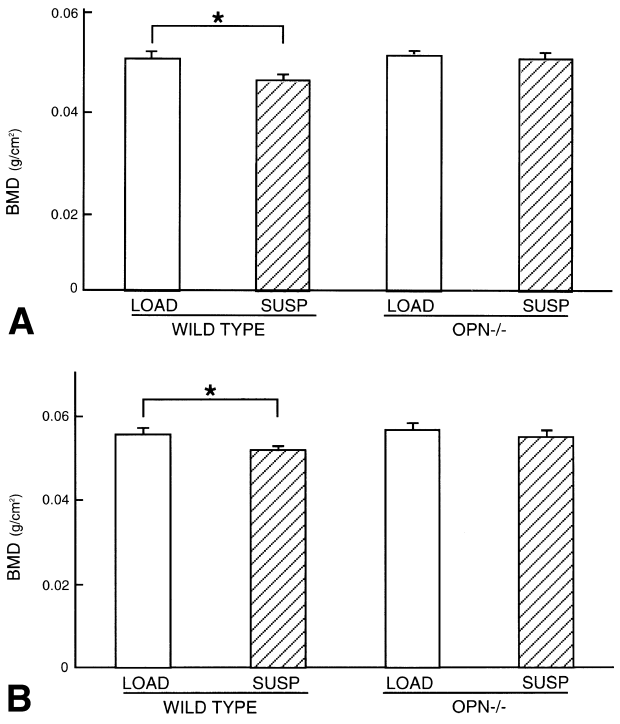

FIG. 3. BMD of the femora and tibias after unloading. DXA was conducted to quantify BMD of the (A) tibias and (B) femora after 4 weeks of either tail suspension (SUSP) or loading (LOAD) in $OPN^{-/-}$ mice ($OPN^{-/-}$) or wild-type mice (WILD TYPE). Data are expressed as means and SEs for wild-type and $OPN^{-/-}$ mice. *Statistically significant difference from respective control ($p < 0.05$).

wild-type group, tail suspension did not decrease BMD levels in the femora and tibias in $OPN^{-/-}$ mice (Figs. 3A and 3B). These observations on both 3D parameters and BMD were not simply the influence of the body weights because no major alteration in body weight was observed during the tail-suspension experiments (data not shown).

DISCUSSION

Our present data revealed that the 3D structures of the trabecular bones were disrupted by unloading in tail-suspended wild-type mice and that the OPN-deficient mice are resistant to such 3D structural alterations including anisotropy. Our DXA data also showed that $OPN^{-/-}$ mice were resistant against loss of bone mineral induced by unloading. These observations indicated that tail-suspension–induced loss of 3D structures as well as BMD required the presence of OPN in the mice.

Traditional trabecular bone morphometry has been conducted in 2D planes,[21] where the structural parameters are either inspected visually or measured from sections, and the third dimension is added based on stereology.[25] To overcome the limitations of the analysis of 2D histological sections, including inability to measure the anisotropic nature of cancellous bone, several 3D analysis techniques have been developed to provide possibilities to measure a variety of 3D structural indices to characterize bone microarchitecture. These techniques facilitate the understanding of the quality of bones and help estimate mechanical properties of bone. Our previous study indicated that $OPN^{-/-}$ mice were resistant to unloading-induced bone loss based on the indirect estimation of the true structures (i.e., 3D structures) using 2D analysis of bone.[20] Thus, to evaluate the true quantitative effect of OPN on unloading-induced bone loss, 3D analysis was conducted in this study using bones of $OPN^{-/-}$ mice subjected to unloading.

3D μCT analysis is a relatively new technique and, therefore, the procedures to analyze quantitatively the trabecular bone structure have not yet been fully standardized.[25] In our 3D μCT analysis, structural indices determined from the microtomography measurements are dependent on the incorporated thresholding procedure. Müller et al. pointed out that it is advantageous to use a uniform threshold for one type of bone to be able to compare results within the site.[25] On the other hand, Feldkamp et al.[30] claimed that a uniform threshold approach is inappropriate for 3D μCT analysis because the X-ray attentuations through the heterogeneous bone structures are not uniform and there may exist trabeculae of varying densities throughout the specimen. Although this issue still remains to be solved, we used a uniform threshold to quantify the 3D structural parameters of bones in our study. In addition, a highly significant correlation between the parameters obtained from conventional histology and those from the 3D μCT was reported.[25] Therefore, although a relatively small number of trabeculae were present in the area measured in our study as shown in Fig. 1, the 3D structural parameters of bones obtained in this study could provide a reasonable estimation of the bone structure based on the most advanced technique of the morphological evaluation.

We observed that the levels of 3D BV/TV, 3D Tb.Th, and 3D Tb.N were significantly reduced after 4 weeks of tail suspension in wild-type mice. On the other hand, these reductions were not observed in $OPN^{-/-}$ mice even after 4 weeks of unloading. It has been proposed that the reduction of trabecular bone volume during osteoporosis is caused by primarily the initial conversion of plate trabeculae to rod trabeculae by the perforation of the trabecular plates.[31] These phenomena are thought to occur because of adaptation of bone to the mechanical stress to which it is subjected. In this study, 3D Tb.Th and 3D Tb.N were measured by using the direct 3D technique, not based on calculation according to the standard plate model. Although these parameters were significantly reduced, the decrease in bone volume induced by unloading was caused by primarily a decrease in Tb.Th (~80% reduction) as opposed to a decrease in Tb.N (~25% reduction) after 4 weeks of unloading in the wild-type mice. In addition, even after 2 weeks of tail suspension, similar results, that is, the reduction in these 3D parameters in wild-type mice and no alterations in $OPN^{-/-}$ mice, were obtained (data not shown).

Anisotropy of the trabecular bones in the metaphyseal regions of the tibias of unloaded mice was measured using μ-CT by accessing the 3D structure. In wild-type mice, in addition to unloading-induced bone loss, the bones became isotropic due to unloading, meaning that the bones could

sense the mechanical stimuli and could alter its properties to adapt the stress to which it is subjected. In $OPN^{-/-}$ mice, neither bone loss induced by unloading nor reduction of the anisotropy of their hindlimbs was observed, indicating that the bones of $OPN^{-/-}$ mice remained anisotropic even after unloading. Therefore, the mice lacking OPN could not sense the changes in mechanical stress to which they were subjected.

Several studies have been tried to prevent this unloading-induced bone loss in tail-suspended animals using antiresorptive agents such as bisphosphonates[32,33] or osteoprotegerin.[34] Although unloading-induced bone resorption was inhibited in these studies, unloading-induced bone formation was not inhibited. On the other hand, in our previous study, unloading-induced bone formation as well as bone resorption were inhibited in the absence of OPN, suggesting that OPN has an important role not only in unloading-induced enhancement of bone resorption but also in unloading-induced suppression of bone formation.[20] Our preliminary in vitro experiments showed that the levels of nodule formations in bone marrow cells were reduced after tail suspension in wild-type mice and they were not reduced in the cells derived from $OPN^{-/-}$ mice after tail suspension compared with those in $OPN^{-/-}$-loaded control mice (data not shown). Further study is necessary to elucidate the mechanisms of OPN actions, that is, as to how osteoblasts and osteocytes could perceive external mechanical stimuli to influence the bones in a 3D environment where these cells exist.

BMD and bone microarchitecture are important determinants for the mechanical properties of cancellous bone. Although BMD alone is a predictor of averaged mechanical properties of cancellous bone, there yet remains unexplained variation in mechanical properties that might be caused by missing information regarding bone microarchitecture.[21] Also, in this study, quantitative area of 3D analysis of bone was limited within the secondary spongiosa of the proximal tibias because of the technical properties of the μCT used. Therefore, to further support the idea that the effect of OPN in this unloading-induced bone loss was not restricted within a particular region, we evaluated the BMD of the whole tibia. Although the reduction of BMD was modest, it was statistically significant. These data further suggest the role of OPN in regulation of the structural properties of bone.

OPN expression in vitro has been observed not only to be enhanced but also inhibited by mechanical stimuli, suggesting the presence of the biphasic nature of OPN gene expression.[14,16] This feature is similar to that in the case of several genes in vascular endothelial cells subjected to mechanical stress.[35] Such effects of mechanical stress on OPN expression appear to be dependent on integrin and microfilament[15,18] but independent of hormonal regulation.[13] Furthermore, OPN secreted by mechanical stress may serve as a stress-sensitive attachment molecule being a ligand of integrin in osteoblasts, osteocytes, and, presumably, osteoclasts.[14,18,19] However, these previous in vitro observations were based on cells plated on flat culture dishes and, thus, may not provide true relationship between mechanical stimulation and bone cells sitting in an in vivo 3D environment. Although our data on the 3D structural analysis of the bone in OPN-deficient mice subjected to tail suspension do not directly explain how OPN may work in vivo, they would provide a base for future studies on how the mechanical stress regulates bone cells in a 3D in vivo environment.

The result of 3D analysis in this study indicated that bones of $OPN^{-/-}$ mice subjected to tail suspension could not alter the 3D morphological structures of trabecular bones to adapt to the new stress (unloading) environment. Overall, our data support the notion that OPN plays a role in the signal transduction pathways of mechanical stress in bone remodeling.

ACKNOWLEDGMENTS

This research was supported by grants 13045011, 13216034, 12557123, and 0930734 from the Ministry of Education, Science, Sports, and Culture of Japan; grants from Core Research for Evolutional Science and Technology (CREST) of Japan Science and Technology Corp. (JST); grant 96I00205 from the Japan Society for the Promotion of Science (JSPS); a grant from the National Space Development Agency of Japan (NASDA); a grant from Tokyo Biochemistry Research Foundation (TBRS); and U.S. National Institutes of Health (NIH) grants AR44434, ES06897 (to D.T.D.), and CA72740 (to S.R.R.).

REFERENCES

1. Rodan GA, Martin TJ 2000 Therapeutic approaches to bone diseases. Science **289:**1508–1514.
2. Goldstein SA, Goulet R, McCubbrey D 1993 Measurement and significance of three-dimensional architecture to the mechanical integrity of trabecular bone. Calcif Tissue Int **53**(Suppl 1)**:**S127–S132.
3. Huiskes R, Ruimerman R, van Lenthe GH, Janssen JD 2000 Effects of mechanical forces on maintenance and adaptation of form in trabecular bone. Nature **405:**704–706.
4. Denhardt DT, Guo X 1993 Osteopontin: A protein with diverse functions. FASEB J **7:**1475–1482.
5. Rodan GA 1995 Osteopontin overview. Ann NY Acad Sci **760:**1–5.
6. Denhardt DT, Noda M 1998 Osteopontin expression and function: Role in bone remodeling. J Cell Biochem Suppl **30–31:** 92–102.
7. Liaw L, Birk DE, Ballas CB, Whitsitt JS, Davidson JM, Hogan BL 1998 Altered wound healing in mice lacking a functional osteopontin gene (spp1). J Clin Invest **101:**1468–1478.
8. Rittling SR, Matsumoto HN, McKee MD, Nanci A, An XR, Novick KE, Kowalski AJ, Noda M, Denhardt DT 1998 Mice lacking osteopontin show normal development and bone structure but display altered osteoclast formation in vitro. J Bone Miner Res **13:**1101–1111.
9. Rittling SR, Denhardt DT 1999 Osteopontin function in pathology: Lessons from osteopontin-deficient mice. Exp Nephrol **7:**103–113.
10. Yoshitake H, Rittling SR, Denhardt DT, Noda M 1999 Osteopontin-deficient mice are resistant to ovariectomy-induced bone resorption. Proc Natl Acad Sci USA **96:**8156–8160.
11. Asou Y, Rittling SR, Yoshitake H, Tsuji K, Shinomiya K, Nifuji A, Denhardt DT, Noda M 2001 Osteopontin Facilitates

Angiogenesis, Accumulation of Osteoclasts, and Resorption in Ectopic Bone. Endocrinology **142:**1325–1332.
12. Kubota T, Yamauchi M, Onozaki J, Sato S, Suzuki Y, Sodek J 1993 Influence of an intermittent compressive force on matrix protein expression by ROS 17/2.8 cells, with selective stimulation of osteopontin. Arch Oral Biol **38:**23–30.
13. Harter LV, Hruska KA, Duncan RL 1995 Human osteoblast-like cells respond to mechanical strain with increased bone matrix protein production independent of hormonal regulation. Endocrinology **136:**528–535.
14. Klein-Nulend J, Roelofsen J, Semeins CM, Bronckers AL, Burger EH 1997 Mechanical stimulation of osteopontin mRNA expression and synthesis in bone cell cultures. J Cell Physiol **170:**174–181.
15. Toma CD, Ashkar S, Gray ML, Schaffer JL, Gerstenfeld LC 1997 Signal transduction of mechanical stimuli is dependent on microfilament integrity: Identification of osteopontin as a mechanically induced gene in osteoblasts. J Bone Miner Res **12:**1626–1636.
16. Meazzini MC, Toma CD, Schaffer JL, Gray ML, Gerstenfeld LC 1998 Osteoblast cytoskeletal modulation in response to mechanical strain in vitro. J Orthop Res **16:**170–180.
17. Miles RR, Turner CH, Santerre R, Tu Y, McClelland P, Argot J, DeHoff BS, Mundy CW, Rosteck PR Jr, Bidwell J, Sluka JP, Hock J, Onyia JE 1998 Analysis of differential gene expression in rat tibia after an osteogenic stimulus in vivo: Mechanical loading regulates osteopontin and myeloperoxidase. J Cell Biochem **68:**355–365.
18. Carvalho RS, Schaffer JL, Gerstenfeld LC 1998 Osteoblasts induce osteopontin expression in response to attachment on fibronectin: Demonstration of a common role for integrin receptors in the signal transduction processes of cell attachment and mechanical stimulation. J Cell Biochem **70:**376–390.
19. Terai K, Takano-Yamamoto T, Ohba Y, Hiura K, Sugimoto M, Sato M, Kawahata H, Inaguma N, Kitamura Y, Nomura S 1999 Role of osteopontin in bone remodeling caused by mechanical stress. J Bone Miner Res **14:**839–849.
20. Ishijima M, Rittling SR, Yamashita T, Tsuji K, Kurosawa H, Nifuji A, Denhardt DT, Noda M 2001 Enhancement of osteoclastic bone resorption and suppression of osteoblastic bone formation in response to reduced mechanical stress do not occur in the absence of osteopontin. J Exp Med **193:**399–404.
21. Ulrich D, van Rietbergen B, Laib A, Ruegsegger P 1999 The ability of three-dimensional structural indices to reflect mechanical aspects of trabecular bone. Bone **25:**55–60.
22. Kabel J, Odgaard A, van Rietbergen B, Huiskes R 1999 Connectivity and the elastic properties of cancellous bone. Bone **24:**115–120.
23. Muller R, Hildebrand T, Hauselmann HJ, Ruegsegger P 1996 In vivo reproducibility of three-dimensional structural properties of noninvasive bone biopsies using 3D-pQCT. J Bone Miner Res **11:**1745–1750.
24. Odgaard A 1997 Three-dimensional methods for quantification of cancellous bone architecture. Bone **20:**315–328.
25. Muller R, Van Campenhout H, Van Damme B, Van Der Perre G, Dequeker J, Hildebrand T, Ruegsegger P 1998 Morphometric analysis of human bone biopsies: A quantitative structural comparison of histological sections and micro-computed tomography. Bone **23:**59–66.
26. Ito M, Nakamura T, Matsumoto T, Tsurusaki K, Hayashi K 1998 Analysis of trabecular microarchitecture of human iliac bone using microcomputed tomography in patients with hip arthrosis with or without vertebral fracture. Bone **23:**163–169.
27. Ruegsegger P, Koller B, Muller R 1996 A microtomographic system for the nondestructive evaluation of bone architecture. Calcif Tissue Int **58:**24–29.
28. Muller R, Ruegsegger P 1996 Analysis of mechanical properties of cancellous bone under conditions of simulated bone atrophy. J Biomech **29:**1053–1060.
29. Harrigan TP, Mann RW 1984 Characterization of microstructural anisotropy in orthotropic materials using a second rank tensor. J Mater Sci **19:**761–767.
30. Feldkamp LA, Goldstein SA, Parfitt AM, Jesion G, Kleerekoper M 1989 The direct examination of three-dimensional bone architecture in vitro by computed tomography. J Bone Miner Res **4:**3–11.
31. Parfitt AM, Drezner MK, Glorieux FH, Kanis JA, Malluche H, Meunier PJ, Ott SM, Recker RR 1987 Bone histomorphometry: Standardization of nomenclature, symbols, and units. Report of the ASBMR Histomorphometry Nomenclature Committee. J Bone Miner Res **2:**595–610.
32. Bikle DD, Morey-Holton ER, Doty SB, Currier PA, Tanner SJ, Halloran BP 1994 Alendronate increases skeletal mass of growing rats during unloading by inhibiting resorption of calcified cartilage. J Bone Miner Res **9:**1777–1787.
33. Kodama Y, Nakayama K, Fuse H, Fukumoto S, Kawahara H, Takahashi H, Kurokawa T, Sekiguchi C, Nakamura T, Matsumoto T 1997 Inhibition of bone resorption by pamidronate cannot restore normal gain in cortical bone mass and strength in tail-suspended rapidly growing rats. J Bone Miner Res **12:**1058–1067.
34. Bateman TA, Dunstan CR, Ferguson VL, Lacey DL, Ayers RA, Simske SJ 2000 Osteoprotegerin mitigates tail suspension-induced osteopenia. Bone **26:**443–449.
35. Resnick N, Gimbrone MA Jr 1995 Hemodynamic forces are complex regulators of endothelial gene expression. FASEB J **9:**874–882.

Address reprint requests to:
Masaki Noda, M.D., Ph.D.
Department of Molecular Pharmacology
Medical Research Institute
Tokyo Medical and Dental University
3–10, Kanda-Surugadai 2-Chome
Chiyoda-Ku, Tokyo 101-0062, Japan

Received in original form June 22, 2001; in revised form September 20, 2001; accepted October 25, 2001.